

# Body Posture Identification using Hidden Markov Model with a Wearable Sensor Network

Muhannad Quwaider  
NeEWS Laboratory  
Electrical and Computer Engineering  
Michigan State University  
East Lansing, USA  
[quwaider@msu.edu](mailto:quwaider@msu.edu)

Subir Biswas  
NeEWS Laboratory  
Electrical and Computer Engineering  
Michigan State University  
East Lansing, USA  
[sbiswas@egr.msu.edu](mailto:sbiswas@egr.msu.edu)

## ABSTRACT

This paper presents a networked proximity sensing and Hidden Markov Model (HMM) based mechanism that can be applied for stochastic identification of body postures using a wearable sensor network. The idea is to collect relative proximity information between wireless sensors that are strategically placed over a subject's body to monitor the relative movements of the body segments, and then to process that using HMM in order to identify the subject's body postures. The key novelty of this approach is a departure from the traditional accelerometry based approaches in which the individual body segment movements, rather than their relative proximity, is used for activity monitoring and posture detection. Through experiments with body mounted sensors we demonstrate that while the accelerometry based approaches can be used for differentiating activity intensive postures such as walking and running, they are not very effective for identification and differentiation between low activity postures such as sitting and standing. We develop a wearable sensor network that monitors relative proximity using Radio Signal Strength indication (RSSI), and then construct a HMM system for posture identification in the presence of sensing errors. Controlled experiments using human subjects were carried out for evaluating the accuracy of the HMM identified postures compared to a naïve threshold based mechanism, and its variations over different human subjects.

**Keywords:** Body Sensor Network, Posture Identification, Hidden Markov Model.

## 1. INTRODUCTION

Human health monitoring using both in-body and out-of-body sensors [1][2][3][4] is increasingly emerging as a dominant application framework for the evolving sensor network technology [5][6]. A number of tiny wireless sensors, strategically placed on a patient's body, can create a Wireless Body Area Network (WBAN) [7][8], that can monitor various vital signs, providing real-time feedback to the patient, his or her doctors, and other medical service provider personnel. Many patients diagnostic procures can benefit from such continuous monitoring to be as a part of optimal maintenance of a chronic condition or during supervised recovery from an acute event or surgical procedure.

Permission to make digital or hard copies of all or part of this work for personal or classroom use is granted without fee provided that copies are not made or distributed for profit or commercial advantage and that copies bear this notice and the full citation on the first page. To copy otherwise, or republish, to post on servers or to redistribute to lists, requires prior specific permission and/or a fee.

Permission to make digital or hard copies of all or part of this work for personal or classroom use is granted without fee provided that copies are not made or distributed for profit or commercial advantage and that copies bear this notice and the full citation on the first page. To copy otherwise, to republish, to post on servers or to redistribute to lists, requires prior specific permission and/or a fee.  
BodyNets 2008, March 13-15 Tempe, Arizona, USA  
Copyright © 2008 ICST 978-963-9799-17-2  
DOI 10.4108/ICST.BODYNETS2008.2932

Recent technological advances in wireless networking promise a new generation of wireless sensor networks suitable for many of the health related applications as outlined above.

In this paper we deal with a body posture identification problem in which a wireless network of body-mounted sensors is used for monitoring and identifying the posture of a human subject. The spectrum of postures to be identified may include sitting, lying down, standing, walking, jogging and other physical activities that relate to lifestyle and behavioral factors and play a role in the etiology and prevention of many chronic diseases such as cancer and coronary heart disease. Once developed, such a wearable sensor network for posture identification can be used for patients' physical activity assessment for both surveillance and epidemiologic/clinical research purposes. Such automated instrumentation for physical activity and body posture detection has recently been actively promoted by various health oriented research organizations including the National Institute of Health (NIH) [9].

In a number of existing works [10][11] multi-axes accelerometers are used for the identification of body postures by analyzing the level of acceleration in different body segments, which is a direct indication of physical activity. These mechanisms are shown to work very well for identifying postures such as walking, jogging, and sprinting. However, for applications those require context identification at finer granularities, it is often necessary to differentiate between low-activity postures such as standing, sitting, lying down, and sometimes with even finer granularity such as sitting upright or reclined. For these non activity-intensive postures the traditional accelerometer based solutions do not work well.

For detecting non activity-intensive body postures, we propose a proximity-based sensing solution, in which the instantaneous physical proximity between different body segments is sensed by measuring the relative radio frequency signal strength between body mounted sensors. Information from multiple sensors is then temporally correlated to estimate the orientation of the body segments and the resulting postures. We have also developed a Hidden Markov Model (HMM) based stochastic posture identification system that can compensate for sensing errors that are found to have been caused by subject's clothing, body structure, and the variability in the sensor mounting.

While the proposed framework is general enough to execute the posture detection computation both on and off line as well as on-body and out-of-body, the laboratory system described in this paper performs out-of-body and off-line posture

identification. Extension of the system for on-line and on-body detection is currently being worked on.

## 2. WEARABLE SENSOR NETWORK

A sensor network, as shown in Figure 1, is constructed by mounting multiple sensors in different parts of the body, so that the individual sensors movement can reflect the displacement of the corresponding body segment. Mica2Dot mote radio nodes, operating with 433MHz radio, and its sensor card MTS510 from the Crossbow Inc. [12] are used as the wearable sensor nodes. The Mica2Dot nodes run from a 570mAH button cell with a total node weight of 5.9 grams. In our experiments, each sensor is worn with an elastic band so that the sensor mount orientation does not change during experiments involving heavy activities including walking and running.

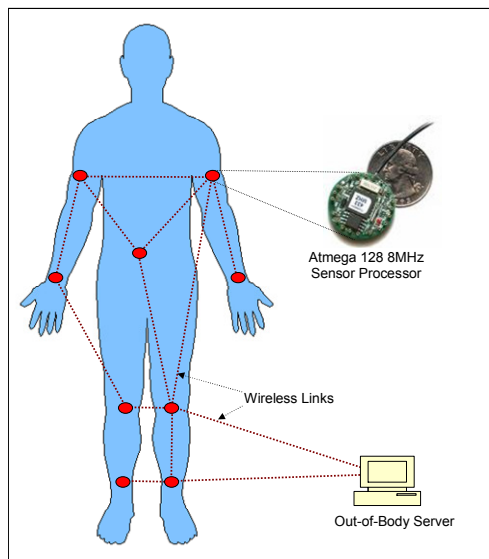


Figure 1: Wearable wireless sensor network

As shown in the diagram, the wearable sensor nodes form an ad hoc sensor network with a topology that is dynamically determined based not only on the relative locations of the subject's limbs but also on the wireless link qualities determined by the transmission power and instantaneous link attenuation. Wireless links are also available to transport raw data or processed events from the body network to an external processing server. A MICA2 radio node with custom-built serial interface to run RS232 protocol has been used for collecting data and events from the body network and send it to a Windows based PC used as the processing server.

### 2.1 Sensor Modalities

Two sensor modalities, namely, acceleration and relative proximity are used for the developed system. A two-axes [10] piezoelectric accelerometer in the Mica2Dot sensor card is used for detecting the changes in body movements. Since acceleration is proportional to the net external force, it provides a very direct indication of the energy expenditure [10] due to the involving physical activities.

The proximity between the sensor nodes in Figure 1 is the second sensor modality that is measured using received signal

strength indication (RSSI) of the radio signal. Each sensor is set to periodically send a *Hello* message to all its neighbors with a preset transmission power that is enough to reach all sensors on the body. Based on those *Hello* packets, each node creates and maintains a local neighbor table consisting of the RSSI values for all its individual radio neighbors. In addition to constructing the local topology information, this way each node maintains a measure of the relative proximity for its neighbor nodes. It was experimentally found that a *Hello* interval of 2.5 sec, and transmissions at 10% of the maximum power was sufficient for the proposed proximity detection mechanism to work.

### 2.2 Sensor Placement

Considering the practical ease of wearing and to capture high level of acceleration it was decided that the sensors will be mounted at the body extremities including the ankles, wrists and head (on a cap). To capture the limb movements using the proximity information, additional sensors are placed on the thighs, waist and upper arms. Note that while more sensors provide richer set of data to work with, it also makes the overall sensor wearing process cumbersome and impractical. Therefore, a key objective of the system design is to achieve high posture identification success rate with as few sensor nodes as possible.

With the general sensor placement guideline as outlined above, the following specific placement issues were needed to be resolved [11]. First, the number of mounted sensors should be minimized while capturing sufficient diversities for both the chosen modalities. Through extensive experimentation with different subject individuals it was found that two sensors on both the upper arms and two sensors on the thighs provide enough information diversity (for both acceleration and proximity) for them to be applicable to our proposed posture identification techniques.

Second, it was found that due to the variability of the inter-node link quality, caused primarily by body movements, antenna mis-orientation, and signal blockage by clothing material, not only the network topology becomes unpredictably dynamic, but the proximity information indicated by the RSSI values can also vary over a very large range. This has the potential for introducing serious inaccuracies in the posture identification unless specific measures are taken to suppress the effects of such measurement errors. We use a Hidden Markov Model to specifically address these measurement errors and variability. Choosing the appropriate transmission power for the sensors is also a design issue that needs to be dealt with.

## 3. POSTURE IDENTIFICATION USING ACCELEROMETRY

In this paper, we attempt to identify four body postures, namely, SIT, STAND, WALK and RUN, which represent both activity intensive and non-intensive scenarios. We develop controlled experiments in which human subjects are given pre-determined sequence of those four postures to follow, and the wearable sensor network is used for collecting both accelerometer and proximity data for out-of-body and off-line post processing. Postures, identified using our proposed detection algorithms, are then temporally correlated with the actual sequence given to the subjects for evaluating the identification accuracy.

Figure 2 shows the accelerometer readings (normalized by the gravitational acceleration  $g$ , which is  $9.81 \text{ m/s}^2$ ) corresponding to

a subject's activity from a single sensor, while the subject was following a controlled posture sequence of {SIT, STAND, WALK, RUN, STAND, SIT, STAND, WALK, RUN, STAND, SIT}, each lasting for 60 seconds. A sampling rate of 20 Hz has been used for obtaining reading from the accelerometers. The numbers in the figure correspond to the average of the acceleration recorded in both the axes of the used sensor.

The figure shows as to how the acceleration reading increases from the non activity intensive postures such as SIT and STAND to the activity intensive postures such as WALK and RUN. The readings for SIT and STAND, however, are almost the same due to the absence of any major physical activity in both the postures.

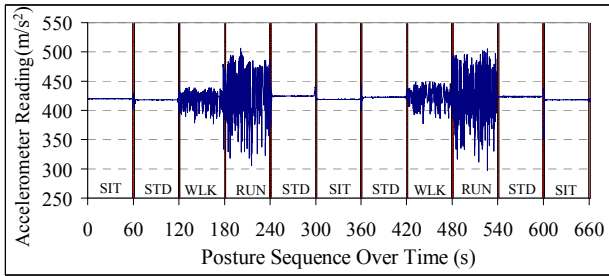


Figure 2: Accelerometer readings in different postures

The frequency domain representation of the collected accelerometer data is presented in Figure 3 for all four postures individually. The graph for WALK, for example, is plotted by applying Fourier Transform to the cumulative acceleration data from all the WALK states as shown in Figure 2. Same applies to the other postures as well.

Observe that while the graphs for WALK and RUN demonstrate a noticeable presence of frequency components in the range 0 to 0.1, the ones for SIT and STAND are almost flat over the entire frequency spectrum. The difference in the peak values for WALK and RUN indicate the difference of activity levels in these two postures. These peak values, coupled with suitably chosen thresholds, can be used for identification and differentiation between the WALK and RUN postures.

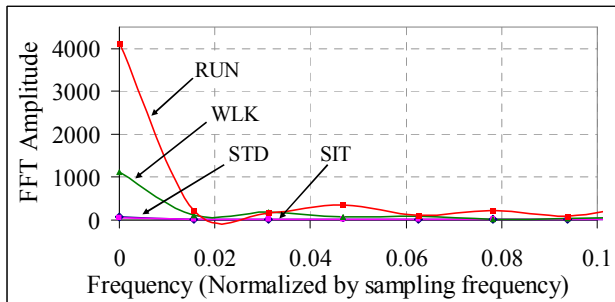


Figure 3: Frequency domain view of the acceleration reading

The frequency domain data can be also used for identification of a low activity state, but as shown in Figure 3, it is likely to fail to differentiate between SIT and STAND due to the lack of any noticeable difference in their respective frequency domain behavior. This clearly demonstrates the inability of the accelerometer based approaches for low activity posture identification.

Figure 4 summarizes the sensing scope for the four targeted postures in this paper. It is shown that while accelerometry is

capable of identifying WALK and RUN, it is not sufficient for the low activity postures. The key idea in this paper is to add a second sensing modality, namely, physical proximity, and its associated analysis techniques for enabling a wearable sensor network to identify all four targeted postures.

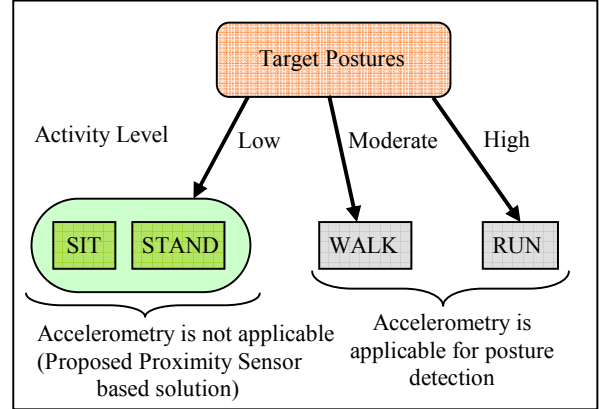


Figure 4: Posture identification using multi-modality sensing

## 4. USING PROXIMITY INFORMATION

As described in Section 2.1, the radio signal strength (RSSI) extracted from the mutual *Hello* messages among the sensor nodes are used as indications of relative sensor proximity in our developed network. Since this proximity information reflects the relative positions of different body parts, it can be used for differentiating postures which are not differentiable using activity information from the accelerometer sensors. In the SIT posture, for instance, the average distance between all body mounted sensors is expected to be smaller than that when a subject is in STAND posture. This idea is particularly implementable since the required proximity information for low activity posture differentiation is needed only in a relative sense without requiring its absolute values.

In this section we provide experimental details for a simple threshold based mechanism for identifying the SIT and STAND postures using proximity as a sensor modality. As shown in Figures 2, 3, and 4, since the acceleration information by itself is sufficient for detecting the WALK and RUN, we propose that the proximity information be used to differentiate between SIT and STAND when a low activity situation is detected from the acceleration data. In the rest of the paper we present experiments and methods to identify SIT and STAND using the sensed proximity data.

### 4.1 Posture Modeling and Generation

The sit-stand behavior of a subject in our experiments is modeled as a Markov process in which the subject's posture transitions assume to follow a memory less process [13]. The transition probabilities across the postures (see Figure 5) represent the subject's behavior that remains stationary for certain time intervals. The transition matrix  $A$  remains fixed during a stationary interval and can vary across such intervals based on specific subject individual and his or her nature and place of work.

In the following experiments we generate a sequence of 50 states of SIT and STAND using the probability transition matrix:

$$A = \{a_{ij}\} = \begin{bmatrix} 0.7 & 0.3 \\ 0.5 & 0.5 \end{bmatrix},$$

where state-1 is SIT and state-2 is STAND. A subject is handed out the resulting posture sequence (S, S, S, S, T, T, S, S, T, T, T, S, T, T, T, S, S, S, S, S, S, T, S, T, T, T, T, T, T, T, T, S, S, S, T), where S represents SIT and T represents STAND, and is instructed to follow the sequence with 10sec being spend in each posture, thus the entire experiment lasting for 500 sec.

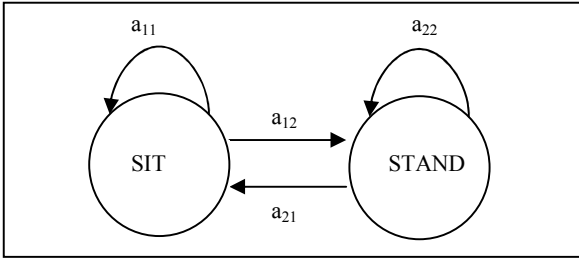


Figure 5: Markov process modeling of SIT-STAND behavior

Four RSSI based proximity sensors are mounted on the subject's body – two on the two upper arms and two on the two front thighs. By interpreting the *Hello* messages, each sensor maintains its current connectivity and RSSI values with all other sensors. The resulting RSSI values are then collected on an out-of-body compute server and averaged to represent the mean instantaneous relative distance between the subject's body segments those are mounted with the sensors.

## 4.2 Threshold based Identification

The average RSSI values (in dB) are plotted in Figure 6 for the entire 500 sec duration of the experiment. The figure also shows the actual posture state that the subject was in during each 10 sec. slot. In these reading, high RSSI dB values indicate low received radio signal strength, and a low RSSI value indicates high received radio signal strength. The following observations should be made. First, the average RSSI has an overall trend to be high for the SIT postures and low for the STAND posture. This is consistent since the body parts are generally closely situated during sitting, and further apart while standing.

Second, while generally maintaining this trend, there are lots of anomalies observed. These anomalies are found to be caused by several factors including radio blockage by the clothing material, unintentional change of sensor and antenna orientations, and other imperfections in sensor mounting.

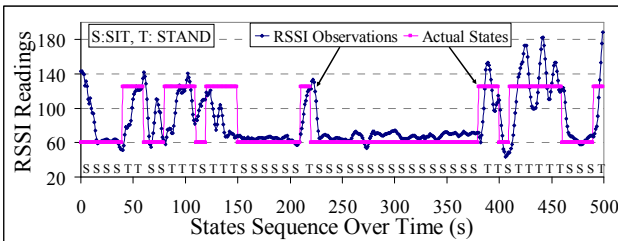


Figure 6: Posture estimation using RSSI (in dB) thresholds

In spite of these anomalies in the average RSSI data, it is possible to identify the SIT and STAND postures by using a

carefully chosen RSSI threshold somewhere between the minimum and the maximum values of the observed data. In Figure 7, we report the effectiveness of such posture identification using different threshold values. The identified posture for a given RSSI threshold is compared with the subject's actual state for computing the success rate as reported in the Figure. Such success or match rates are presented for different threshold values and for different individuals participated as experimental subjects. All three individuals in these experiments were asked to follow the same controlled posture sequence used in Figure 6 for several rounds, before the identification performance were computed.

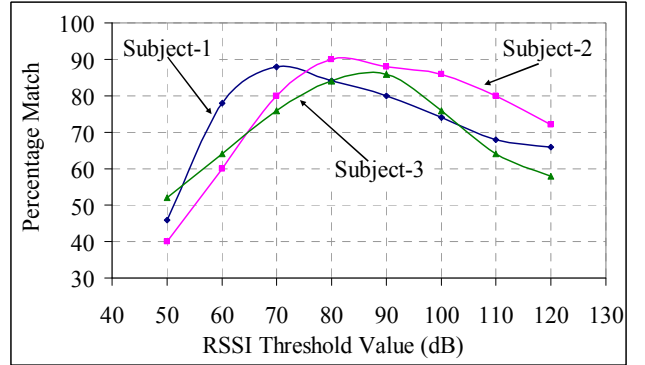


Figure 7: Posture detection success with varying RSSI thresholds

Observe that in spite of the errors contributed by sensor and antenna mis-orientation, and radio signal blockage by clothing material, this simple threshold based mechanism can detect the SIT and STAND postures with up to approximately 90% accuracy. However, since the identification success rate is heavily sensitive to the RSSI threshold, choosing the right threshold is an important design step for this mechanism to work.

A potentially more restricting aspect is that the optimal threshold is also sensitive to the individual subjects' physical and motor aspects during his or her postures. For example, while an RSSI threshold of 70 yields the best identification accuracy for subject-1, the performance for subject-3 maximizes at 86% for a threshold 90. In fact, at the RSSI threshold of 70, for subject-3 the system delivers a poor posture identification rate of only 75%.

These results allude to a practical limitation of the threshold based posture identification in terms of the need for person specific threshold dimensioning. Other experiments further indicated that the optimal threshold value can change even for an individual based on his or her behavioral changes over time. In the next section we develop a Hidden Markov Model (HMM) based mechanism for adaptive and person-independent posture detection.

## 5. CAPTURING STATIONARY BEHAVIOR USING HIDDEN MARKOV MODEL

The inability of the simple threshold based mechanism to handle the degraded quality of proximity sensor data stems from the fact that the identification process does not leverage the stationary nature of human behavior over certain time intervals.

To address this limitation, we adopt a stochastic posture identification solution that attempts to leverage the stationary

nature of the human behavior by modeling the posture state machine as a Hidden Markov Model (HMM) [14].

The key concept of the HMM [14] are as follows. A stochastic process is represented by a discrete time Markov Chain consisting of multiple states which are *hidden* from an observer in the sense that an observer cannot directly determine which state the system is in at any given point in time. However, a number of observable parameters that stochastically represent the states are visible to the observer. The idea of HMM formulation is that if the state transition probability matrix and the observation generation probabilities are known (or measurable) to the observer, the latter can estimate the current state of the Markov Chain. Using HMM it is also possible to compute the probability of occurrence of a specific state sequence [15][16][17][18].

## 5.1 HMM Mapping

The posture identification problem with our novel proximity sensing framework is mapped as an HMM formulation as follows.

**Posture State Space:** As shown in Figure 8,  $N$  postures are modeled as  $N$  hidden states with the entire state space represented by  $S = \{S_1, S_2, \dots, S_N\}$ . In this specific case  $N = 2$  for postures SIT and STAND.

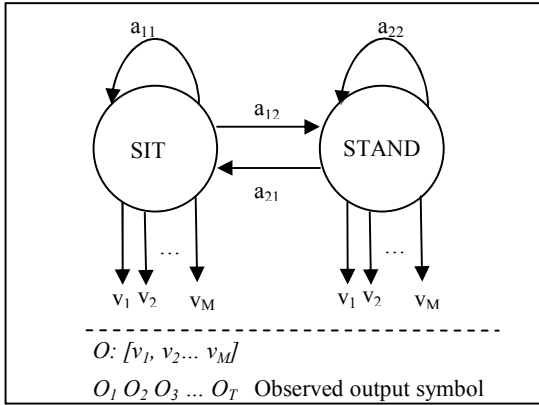


Figure 8: Posture state machine with hidden states

**Observation:** At each state there are  $M$  distinct observable parameters that are represented by a vector  $O = \{v_1, v_2, \dots, v_M\}$ . Each  $v_m$  ( $m=1, 2, \dots, M$ ) can take one of multiple possible values. Observation made at time instant  $t$  is represented as  $O_t$ .

At any given time, the radio RSSI values from the sensor are used to construct the  $O_t$  vector, in which each  $v_m$  is a binary variable which can be either '0' or '1'. The peak-to-peak RSSI range (see Figure 6) is divided into  $M$  equal windows, and then depending on which window the current RSSI value falls in, the corresponding  $v_m$  is set to '1'. The rest of the  $v_m$ 's are set to '0'.

Note that the value of  $M$  determines the granularity of observation, which in turn, is expected to influence the quality of the hidden state identification. We have experimented with  $M$  ranging from a small value of 2 (very coarse granularity) to a large value of 10 (very fine granularity observation).

As indicated in Figure 8, the parameter  $O_t$  represents the observation vector at time slot  $t$ , with  $T$  as the final observations in an experiment. In all our experiments the value of  $T$  is 50. In other words, 50 observations, each corresponds to a state lasting for 10 seconds, are generated to feed into the HMM estimation system.

**Transition Probability Matrix:** The posture transition probability matrix is represented as  $A = [a_{ij}]$ , where

$$a_{ij} = p(q_t = S_j | q_{t-1} = S_i), \quad 1 \leq i, j \leq N \quad (1)$$

$A$  is an  $N \times N$  matrix, and  $q_t$  denotes the actual posture at time  $t$ . The parameter  $a_{ij}$  represents the probability that the next posture is  $j$ , given the current posture of the subject is  $i$ .

**Observation Probability Matrix:** This is represented by  $B = [b_{jm}]$ , in which

$$b_{jm} = p(O_t = [v_1 = 0, \dots, v_m = 1, \dots, v_M = 0] | q_t = S_j), \quad 1 \leq m \leq M \quad (2)$$

$B$  is an  $N \times M$  matrix, and  $O_t$  represents the observation vector at time slot  $t$ . The parameter  $b_{jm}$  represents the probability that in posture state  $j$ , the element  $v_m$  in the observation vector  $O_t$  is '1' and the rest of the elements are all zero.

**Initial State Distribution:** This is represented by a vector  $\pi = [\pi_i]$  of length  $N$ , so that:

$$\pi_i = p(q_0 = S_i), \quad 1 \leq i \leq N \quad (3)$$

The quantity  $\pi_i$  represents the probability that the posture Markov chain is initialized at state  $i$ , by definition,  $\sum_{i=1}^N \pi_i = 1$ .

Based on the above definitions, a system, modeled using HMM, can be fully specified by the parameters  $A$ ,  $B$  and  $\pi$  which are represented together as a tuple:

$$\lambda = (A, B, \pi) \quad (4)$$

Using the HMM derivations shown in Appendix A.1, we first compute the individual probabilities of the system being in each possible posture state at a given time. As shown in the derivation, these probabilities depend on the system's  $\lambda$ , and the observation sequence  $\{O_1 O_2 O_3 \dots O_T\}$ . After the probabilities are computed, the posture state identification is accomplished by finding the most likely state, which is the one with the highest current probability.

## 5.2 Experimental Results

In this section we describe the performance of HMM based posture identification and its performance comparison with the threshold based approach. The same transition probability matrix  $A = \{a_{ij}\} = \begin{bmatrix} 0.7 & 0.3 \\ 0.5 & 0.5 \end{bmatrix}$ , as used for the previous

experiments, is used for generating a posture sequence to be followed by the subjects. Like in the previous experiments, only two posture states SIT and STAND are used. Note that for the results in this Section, the  $A$  matrix used for posture sequence generation is also used for the HMM model formulation. In other words, it is assumed that the  $A$  matrix used for HMM is already trained.

The observation probability matrix  $B$  is constructed by computing the  $b_{jm}$  probabilities (see Equation 2) from observed RSSI values for known posture states. During an initial set of known states, the  $B$  matrix is first computed, and then the actual posture identification process was initiated. This initial period is referred to as an *observation calibration phase*.

As for the Initial State Distribution matrix  $\pi$ , we have used [1, 0] for all the results presented here. This means that all the experiments are initiated with the SIT state. These  $A$ ,  $B$  and  $\pi$  matrices constitute the HMM system parameter  $\lambda$ .

The observation sequence  $\{O_1 O_2 O_3 \dots O_T\}$  is constructed by first collecting the RSSI values from on-body proximity sensors, and then quantizing them into one of  $M$  windows to form the  $v_m$  ( $m = 1, 2, \dots, M$ ) elements within each observation vector. We have experimented with different observation granularity vector  $M$  ranging from 2 to 10.

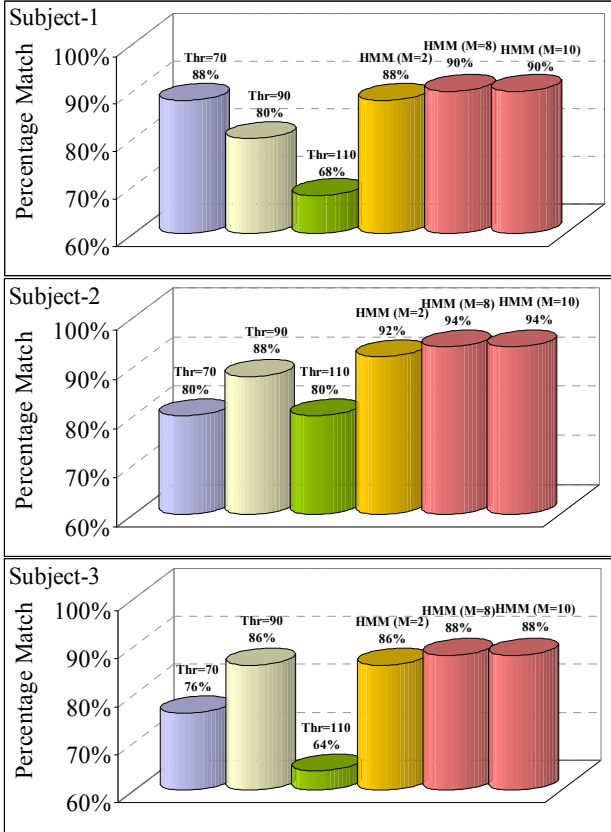


Fig. 9: Posture detection performance using HMM

After the observation sequence is constructed, the HMM derivations, shown in Appendix A.1, are used to identify posture states using the system parameter  $\lambda$  and the observation sequence  $\{O_1 O_2 O_3 \dots O_T\}$ .

State identification performance with HMM in comparison with the threshold based mechanism is presented in Figure 9. As done before, the success rates are measured by comparing the detected states with the actual states from the generated posture sequence using transition probability matrix  $A$ .

The success rate for posture identification using HMM is reported with three different observation granularities corresponding to  $M = 2, 8$  and  $10$ . The following observations are to be made from Figure 9. First, the HMM approach delivers better state match rates (e.g. 92% to 94% identification success for subject-2) compared to the best case performance (88% identification success for subject-2) using the threshold based mechanism, that is with an optimal RSSI threshold of 90 dB.

Second, higher observation granularity (larger  $M$ ) for HMM provides better posture detection rate, with performance saturation occurring beyond around  $M = 8$ . Third, once a sufficiently large observation granularity (e.g.  $M = 10$ ) is chosen for HMM, unlike in the threshold based scheme, there is no optimal parameter dimensioning is needed. This is a significant advantage in terms of implementation feasibility. Finally, with similarly large observation granularities, the HMM continues to provide superior posture identification performance in a subject-independent manner. This further reinforces the practicality of the mechanism in not having to dimension any individual specific parameter which may cause significant performance variation as observed for the threshold based mechanism.

### 5.3 Automatic Observation Calibration

For the results presented in Section 5.2, the observation probability matrix  $B$  has been constructed during an observation calibration phase before experimenting with each individual subject. This calibration process (construction of matrix  $B$  based on observations) somewhat compensates for the inconsistencies in the radio RSSI values due to variations in clothing, personal posture specialties and other ambient differences. In fact this calibration process accounts a great deal for the consistently superior performance of HMM compared to the threshold based strategy, as presented in Figure 9.

In this section we implement a self-calibration process of the  $B$  matrix, so that the proposed posture identification mechanism can more practically implemented without having to manually calibrate the  $B$  matrix for each individual subject.

We use the Baum-Welch iterative algorithm [14], for which the key idea is to start with an arbitrarily set initial  $B$  matrix, and then iteratively adjust it based on the stochastic difference between the identified (using HMM) posture state sequence and the expected sequence based on the notion of the state transition matrix  $A$ . Details of the Baum-Welch derivation and the algorithm is included in Appendix A.2.

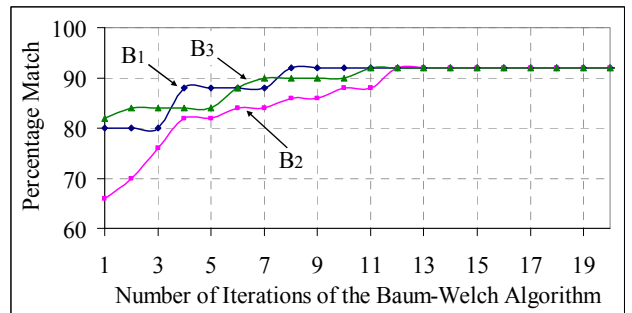


Figure 10: Automatic self-calibration of the  $B$  matrix

Figure 10 demonstrates the performance of this self-calibration process in terms of the posture identification accuracy over multiple iterations. Here we used the observation sequence of subject-2 of the last experiments, with observation granularity  $M = 4$ . Observe that with all three different initial  $B$  matrices, the identification accuracy gradually increases over time with Baum-Welch iterations. For all three cases, the posture identification process started delivering the best performance within 13 iterations. In a deployment sense, this means that after wearing the sensors, the subject should continue with his or her regular behavior for a while for allowing the network to self-calibrate the

HMM  $B$  matrix. After that, the identified posture recording should start.

## 6. SUMMARY AND ONGOING WORK

In this paper we present an experimental framework for a wearable sensor network used for human posture detection. A novel radio frequency based proximity sensing, couple with Hidden Markov Model (HMM) based detection techniques, has been used for detecting low-activity postures that are shown to be not differentiable using the traditional accelerometry based approaches. It was first demonstrated that although a naïve threshold (radio signal) based mechanism can be used for reasonable detection performance, the variation in the proximity information caused by clothing and person-specific behavioral differences require a delicate dimensioning of the used threshold values for consistent posture detection performance across various individuals. To avoid this, an HMM based detection process is applied with observation self-calibration using the Baum-Welch algorithm. It was shown that the HMM method with our novel proximity sensing modality is able to consistently deliver significantly better detection performance than the threshold based mechanism in a more individual-independent manner.

Ongoing work on this topic includes: 1) development of a real-time and on-body posture detection system, 2) integrating proximity and acceleration data for detecting a wider range of both high-activity and low-activity postures, 3) adjusting the HMM and processing mechanism to adapt for different base behavior (the  $A$  matrix). This should scale the proposed mechanism to scenarios in which the  $A$  matrix used for HMM formulation is not already trained.

## 7. REFERENCES

- [1] S. Bao, Y. Zhang, and L. Shen, "Physiological Signal Based Entity Authentication for Body Area Sensor Networks and Mobile Healthcare Systems," *27th IEEE Conference on Engineering in Medicine and Biology, Shanghai, China, pp. 2455–2458, 2005*.
- [2] B. Lo, S. Thiemjarus, R. King and G. Yang, "Body Sensor Network – A Wireless Sensor Platform for Pervasive Healthcare Monitoring," *Proceedings of the 3<sup>rd</sup> International Conference on Pervasive Computing (PERVASIVE 2005), pp.77-80, May2005*.
- [3] C. Otto, A. Milenkovic, C. Sanders, E. Jovanov, "System Architecture of a Wireless Body Area Sensor Network for Ubiquitous Health Monitoring," *Journal of Mobile Multimedia, Vol. 1, No. 4, pp. 307-326, 2006*.
- [4] A. Milenkovic, C. Otto, E. Jovanov, "Wireless Sensor Networks for Personal Health Monitoring: Issues and an Implementation," *to appear in Computer Communications (Special issue: Wireless Sensor Networks: Performance, Reliability, Security, and Beyond), Elsevier, 2006*.
- [5] M. Moh, B. Culpepper, L. Dung, T.-S. Moh, T. Hamada, and C.-F. Su, "On Data Gathering Protocols for In-body Biomedical Sensor Networks," *Proceedings of 48th IEEE Global Telecommunications (GlobeCom), St. Louis, MO, Nov 2005*.
- [6] S.-W. Lee and K. Mase, "Activity and Location Recognition using Wearable Sensors," *Pervasive Computing, vol. 1, no. 3, pp. 24–32, Jul.–Sep. 2002*.
- [7] E. Jovanov, A. Milenković, C. Otto, P. De Groen, B. Johnson, S. Warren, and G. Taibi, "A WBAN System for Ambulatory Monitoring of Physical Activity and Health Status: Applications and Challenges," *Proceedings IEEE Eng Med Biol Soc 4: 3810-3. 2005*.
- [8] E. Jovanov, A. Milenkovic, C. Otto and P. C de Groen, "A Wireless Body Area Network of Intelligent Motion Sensors for Computer Assisted Physical Rehabilitation," *Journal NeuroEng. and Rehab., vol. 2, no. 11, p. 6, Mar. 2005*.
- [9] <http://grants2.nih.gov/grants/guide/pa-files/PA-07-354.html>
- [10] KY. Chen, DR. Bassett Jr, "The Technology of Accelerometry-based Activity Monitors: Current and Future," *Med Sci Sports Exerc;37:S490–500. doi: 10.1249/01.mss.0000185571.49104.82, 2005*.
- [11] A. Ylisaukko-oja, E. Vildjiounaite, J. Mäntyjärvi, "Five-Point Acceleration Sensing Wireless Body Area Network - Design and Practical Experiences," *184-185, ISWC 2004*.
- [12] Crossbow Technology, Inc. <http://www.xbow.com>
- [13] B. Juang, "Maximum Likelihood Estimation for Mixture Multivariate Stochastic Observations of Markov Chains," *AT&T Tech. I., vol. 64, no. 6, pp. 1235-1249, July-Aug. 1985*.
- [14] L. Rabiner, "A Tutorial on Hidden Markov Models and Selected Applications in Speech Recognition," *Proceedings of the IEEE, vol. 77, no. 2, pgs 257 - 285, Feb. 1989*.
- [15] J. Allanach, H. Tu, S. Singh, K. Pattipati and P. Willet, "Detecting, Tracking and Counteracting Terrorist Networks via Hidden Markov Models," *IEEE Aerospace, March 2004*.
- [16] O. Brdiczka, J. Maisonnasse and P. Reignier, "Automatic Detection of Interaction Groups," *ICMI: 32-36, 2005*.
- [17] V. Nair and J. Clark, "Automated Visual Surveillance using Hidden Markov Models," *International Conference on Vision Interface, pp. 88 – 93, 2002*.
- [18] L. Wang, M. Mehrabi, and E. Kannatey-Asibu, Jr. "Hidden Markov Model-based Tool Wear Monitoring in Turning," *Journal of Manufacturing Science and Engineering, Volume 124, Issue 3, pp. 651-658, August 2002*.

## A. APPENDIX

### A.1 Posture Detection using HMM

The probability of observing a given sequence  $O = \{O_1, O_2, \dots, O_T\}$  of length  $T$  time steps is represented as  $P(O|\lambda)$ , and can be evaluated using the forward-backward procedure [16], as follows:

$$P(O|\lambda) = \sum_{i=1}^N \alpha_T(i), \quad (A.1)$$

where  $\alpha_T(i)$  is referred to as forward variable, and defined as:

$$\alpha_t(i) \equiv P(O_1, O_2, \dots, O_t, q_t = s_i | \lambda), \quad 1 \leq i \leq N \quad (A.2)$$

It represents the probability that the partial sequence  $O_1, O_2, \dots, O_t$ , until time step  $t$ , has been observed and the current posture state at time  $t$  is  $S_i$ , given the HMM model  $\lambda$ .  $\alpha_t(i)$  is a vector of dimension  $N$  (which is the total number of possible states). Another variable  $\beta_t(i)$ , referred to as backward variable, is defined as:

$$\beta_t(i) \equiv P(O_{t+1}, \dots, O_T | q_t = s_i, \lambda), \quad 1 \leq i \leq N \quad (A.3)$$

This represents the probability that the partial sequence from time step  $(t+1)$  to the end has been observed and the current posture state at time  $t$  is  $S_i$ , given the model  $\lambda$ .  $\beta_t(i)$  is also a vector of dimension  $N$ . Now another variable  $\gamma_t(i)$  is defined such that:

$$\gamma_t(i) = p(q_t = S_i | O, \lambda), \quad (A.4)$$

where  $\gamma_t(i)$  represents the probability of being in state  $S_i$  at time  $t$ , given an observation sequence  $O$ , and the model  $\lambda$ . Equation (A.4) can be expressed in terms of the forward-backward variables as:

$$\gamma_t(i) = \frac{\alpha_t(i) \beta_t(i)}{P(O|\lambda)} = \frac{\alpha_t(i) \beta_t(i)}{\sum_{i=1}^N \alpha_t(i) \beta_t(i)} \quad (A.5)$$

which is a vector of dimension  $N$  at time  $t$ . Using  $\gamma_t(i)$  we can solve for the individually most likely posture state  $q_t$  at time  $t$  [14], as

$$q_t = \arg \max_{1 \leq i \leq N} [\gamma_t(i)], \quad 1 \leq t \leq T \quad (A.6)$$

This  $q_t$  represents the detected posture state at time  $t$ . The results presented in Section 5.2 are computed based on the derivations from Equations A.1 to A.6.

## A.2 Iterative HMM with Automatic Observation Calibration

As proposed in [14][17], it is possible to calibrate the HMM parameters in  $\lambda$  such that the quantity  $P(O|\lambda)$ , representing the conditional probability of an observation sequence (of length  $T$ ) is maximized. In our specific application of self-calibration as discussed in Section 5.3, it is required to adjust the observation probability matrix  $B$  while keeping the other two parameters  $A$  and  $\pi$  in  $\lambda$  constant. The Baum-Welch algorithm [14] is used in our implementation to iteratively obtain an estimate of  $B$  that results in a  $\lambda$  which is guaranteed to locally maximize  $P(O|\lambda)$ .

As defined in Section 5.1, the element  $b_{im}$  in the matrix  $B$  represents the probability that in posture state  $i$ , the element  $v_m$  in the observation vector  $O$  is '1' and the rest of the elements are all zero. The quantity  $b_{im}$  can be computed as:

$$b_{im} \equiv \frac{\sum_{t=1}^T \gamma_t(i)}{\sum_{t=1}^T \gamma_t(i)} \quad (A.7)$$

where the denominator represents the probability that the system is always in state  $i$  with all possible observations. The numerator represents the probability that the system is in state  $i$  with a specific observation such that the element  $v_m$  in the observation vector  $O$  is '1' and the rest of the elements are all zero.

Using Equation A.7 as the iterative step for changing the  $B$  matrix, we have implemented the following algorithm for implementing self-calibration as explained in Section 5.3.

1. Collect observations  $O = O_1 O_2 \dots O_T$
2. Initialize  $\lambda$  using a starting  $B$  matrix with constant  $A$  and  $\pi$
3. Given observation sequence  $O = O_1 O_2 \dots O_T$  and  $\lambda$ , compute:
 
$$\gamma_t(i), \quad \forall 1 \leq t \leq T, \quad 1 \leq i \leq N$$
4. Compute new  $B$  matrix by updating the elements  $b_{im}$  based on Equation A.7
5. Set new  $\lambda_{new}$  using the new  $B$  matrix
6. Compute a new quantity MAXLIKELIHOOD as:
 
$$MAXLIKELIHOOD = \max[P(O_1 \dots O_T | \lambda), P(O_1 \dots O_T | \lambda_{new})]$$
7.  $\lambda = \lambda_{new}$
8. Go to step-3 and repeat till the quantity MAXLIKELIHOOD converges

The fact that the newly estimated  $B$  matrix in Step 4 is computed based on the actual observation sequence, ensures that the estimation would improve the quantity  $P(O|\lambda)$ . This accounts for the monotonically increasing nature of the MAXLIKELIHOOD, as evidenced in Figure 11.

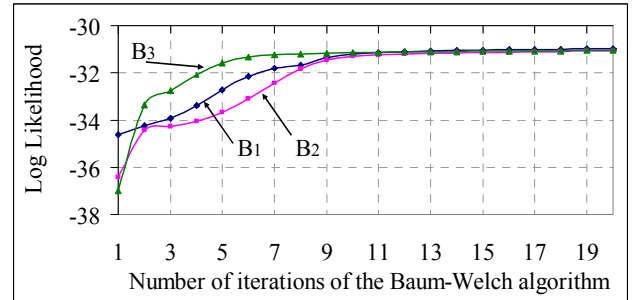


Figure 11: Performance of Baum-Welch iterative algorithm

Figure 11 demonstrates the convergence performance of the Baum-Welch algorithm in terms of the evolution of the log of the quantity MAXLIKELIHOOD. Observe that with all three different initial  $B$  matrices, the MAXLIKELIHOOD monotonically increases over the algorithm iterations, and converges approximately after 13 iterations, which is consistent with what has been reported in Figure 10.